SEISMIC REFRACTION STUDY OF AN EARTHFLOW IN REDWOOD CREEK BASIN, NORTHWESTERN CALIFORNIA

by

Peter Bromirski

A Thesis
Presented to
The Faculty of Humboldt State University

In Partial Fulfillment
of the Requirements for the Degree
Master of Science

July 30, 1989

SEISMIC REFRACTION STUDY OF AN EARTHFLOW
IN REDWOOD CREEK BASIN, NORTHWESTERN CALIFORNIA

by

Peter Bromirski

Approved by the Master's Thesis Committee

8/24/89
Carl Yee, Chairman Date

10/5/89
Lori Dengler Date

10/11/89
Robert Ziemer Date

Oct. 11, 1989
Director, Natural Resources Graduate Program Date

89/WM-169/08/10
Natural Resources Graduate Program Number

Approved by the Dean of Graduate Studies

12/15/89
Robert Willis Date

ABSTRACT

The subsurface structure of an earthflow near Minor Creek in the Redwood Creek basin was studied by seismic refraction. Seismic lines were run both parallel and transverse to the slope near the head and at midslope in the active portion of the flow, and on the flanks adjacent to the active flow.

A three layer structure, defined by two continuous seismic velocity boundaries, was found throughout the earthflow. A 1.0 to 2.5 m thick surface layer was observed on all lines run with a velocity typical of dry unconsolidated and uncompacted material. The base of this layer probably represents the depth of the water table.

The second layer velocities varied from 630 to 720 msec^{-1} in the active portion to about 1100 msec^{-1} beneath the flanks. The lower velocity in the active portion may be a result of disruption due to movement.

The deepest boundary varied in depth from 3.5 to 11.5 m. In the active portion of the earthflow, this boundary closely correlates with the base of the shear zone identified from inclinometer data. The seismic velocities of the third layer are 1100 msec^{-1} which suggests that the material is the same as the second layer beneath the flanks. Beneath the flanks, the third layer velocities are about 2100 msec^{-1}, similar to that of fractured, weathered Franciscan bedrock. The absence of this higher velocity material beneath the active portion within the depth range sampled suggests that the location of the earthflow is structurally controlled.

Key Words: shallow seismic refraction, earthflow, landslide, subsurface structure.

TABLE OF CONTENTS

LIST OF TABLES

Table Page

LIST OF FIGURES

Figure Page

INTRODUCTION

Earthflows are complex, slow-moving landslides that have long been recognized as significant sources of sediment for the fluvial systems of northwest California (Janda et al., 1975; Kelsey, 1977). Rotational slumps and the presence of pressure ridges indicating translational movement are common features in the active portions of earthflows. Identifying the location of the vertical and horizontal boundaries of these different morphological components should contribute to the understanding of earthflow movement and hydrologic processes. There have been numerous studies monitoring earthflow movements (Janda et al., 1980; Keefer and Johnson, 1983; Swanston et al., 1983), and several recent studies investigating their hydrologic regimes (Iverson, 1984; Iverson and Major, in preparation; Swanston et al., 1983; Ziemer, 1984). These studies have associated earthflow movement with an increase in pore water pressure. Due to the size of these features, their complex mode of movement, and the sampling methods employed, previous studies have been unable to determine whether structural controls are present or investigate the continuity of the failure zone over a large scale.

The purpose of this study was to locate the failure surface of an active earthflow using seismic refraction techniques, and to map its topography in several areas of an earthflow near Minor Creek in northern California (Figure 1). The Minor Creek earthflow complex has been heavily monitored for several years. Transverse stakelines, rain-gage measurements, water-discharge gaging and sediment-discharge sampling of major drainage gullies, and extensiometer measurements have been taken for different periods since 1973, with the results reported in studies by Harden et al. (1978), Janda et al. (1980), and Nolan and Janda (in preparation). The availability of the inclinometer data for comparison with the seismic results was a primary reason for the Minor Creek site selection.

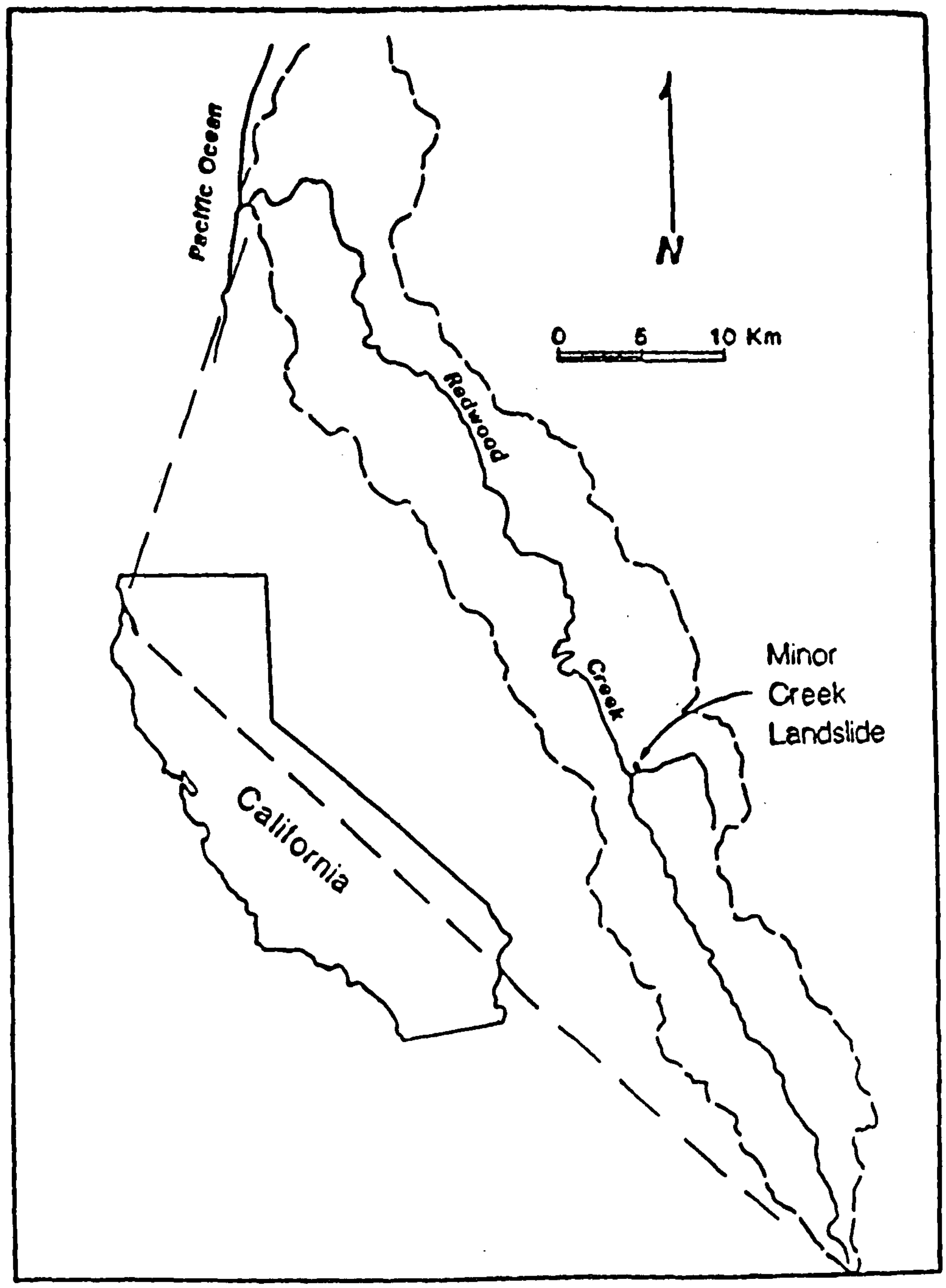

Figure 1. Location of Redwood Creek drainage basin and Minor Creek landslide in northwestern California (after Iverson, 1984)

There are several potential advantages of seismic techniques over drilling for locating subsurface boundaries. The placement of inclinometer tubes in active earthflows is a difficult proposition, with drilling equipment access a major problem. Monitoring the inclinometer tubes for at least several months is generally required in order to identify the depth of the shear zone at point locations. In contrast, shallow refraction equipment is portable and field time for data collection is considerably less than for drilling and monitoring inclinometer holes. In addition, the refraction technique can locate and determine the continuity of material boundaries over entire transects by changes in seismic velocity.

Movement of an initially stable hillslope should result in changes in its bulk properties due to material disruption, which would make the inactive base of the earthflow detectable as a seismic velocity boundary. Since seismic wave velocity depends on the elastic properties of the material, the vertical and spatial distribution of velocity zones also gives information about the physical characteristics of the earthflow material.

SITE CHARACTERISTICS

The Minor Creek earthflow is located in the Redwood Creek basin, northwestern California (Figure 1). The main body of the landslide is about 760 m long and varies from about 50 to 150 m in width over an elevation change of 220 m (Figure 2). The toe of the earthflow is being undercut by Minor Creek, a perennial tributary of Redwood Creek.

The Redwood Creek basin is primarily composed of tectonically accreted Franciscan geologic terrain (Janda, 1979). The rocks of the Minor Creek landslide belong to the Incoherent Unit of Coyote Creek, a part of the Cretaceous section of the

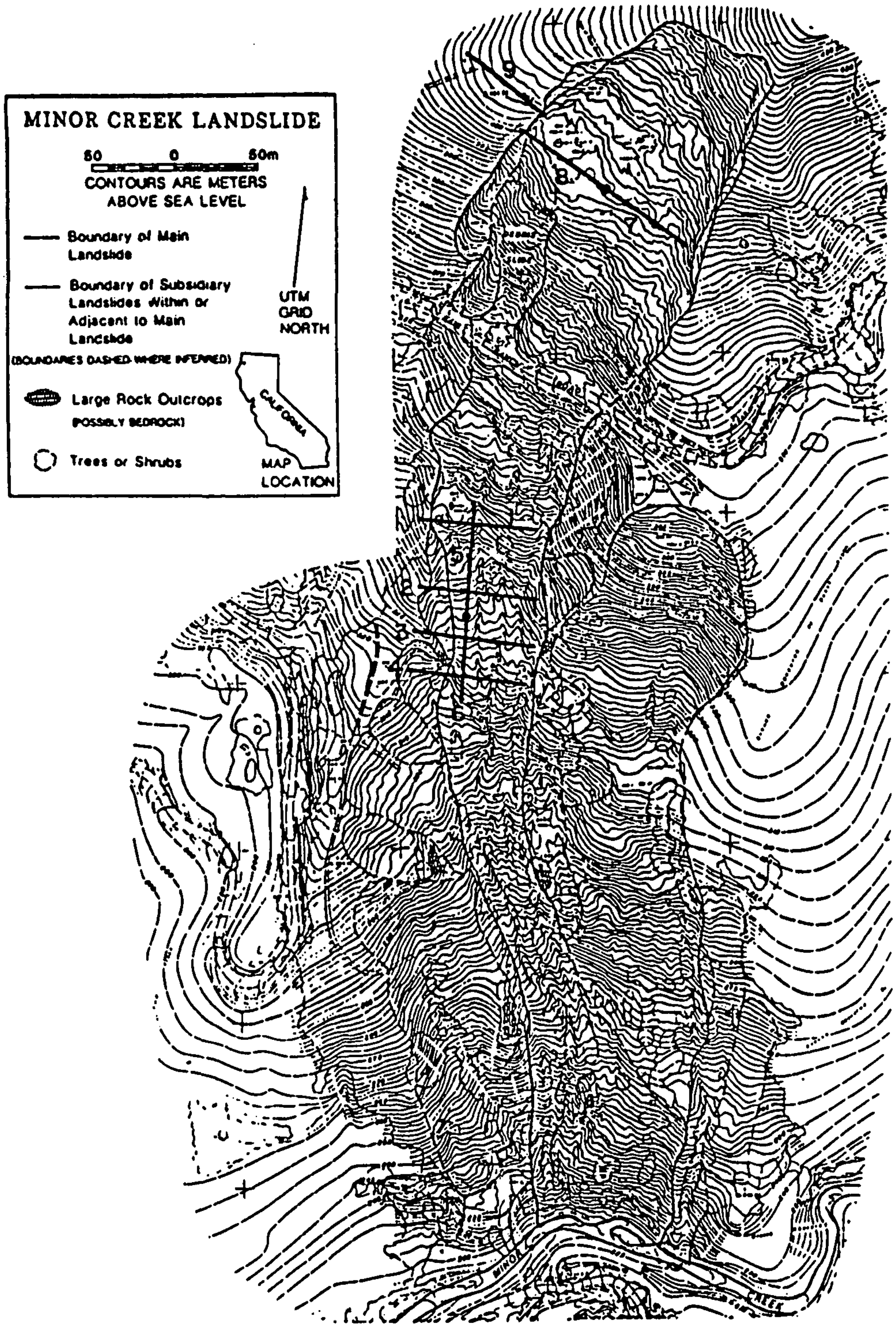

Figure 2. Topographic map showing surface relief and major morphological features of Minor Creek landslide. Heavy straight lines indicate seismic line locations. (after Iverson, 1984)

Franciscan assemblage (Harden et al., 1982). The earthflow is composed of extensively sheared and weathered bedrock material, which contains many granule-size to boulder-size fragments in a clay-rich matrix. Iverson (1984) reports that borings indicate the matrix extends to depths greater than 17 m in parts of Minor Creek landslide.

The surface morphology consists of both relatively smooth, unbroken ground on the inactive flanks and hummocky, broken terrain in the main body. Well defined head and lateral scarps delineate the active region. In several places, large outcropping blocks of rock seem to support and control the location of the lateral scarps. Isolated, small, stable-appearing areas can be seen within the active portion. Bair Ranch Road crosses the landslide about 200 m from the head scarp (Figure 2). An extensive gully system, beginning about 100 m below the road, provides surface drainage from the lower part directly into Minor Creek.

Stake line surveys since 1973 show average surface movement rates to be about 0.5 myr^{-1}, with somewhat larger localized episodic pulses and considerably greater movement near the toe (Iverson, 1984). Iverson concluded that data from all stake lines shows that the central portion of the main landslide mass moves primarily as a rigid body.

Six inclinometer tubes were initially installed in and adjacent to the active portion of the earthflow in 1978 by the U. S. Geological Survey in cooperation with the U. S. Forest Service. An additional nine tubes were installed by Iverson (1984) in 1982 as part of a hydrologic study. The inclinometer method identifies differential motion between depth elements in the slide mass by comparison of repeated tilt measurements over time of tubes placed approximately vertically in the ground (Swanston et al., 1983). Inclinometer results for the central portion of the main landslide indicate considerably smaller movement rates within the slide mass, with

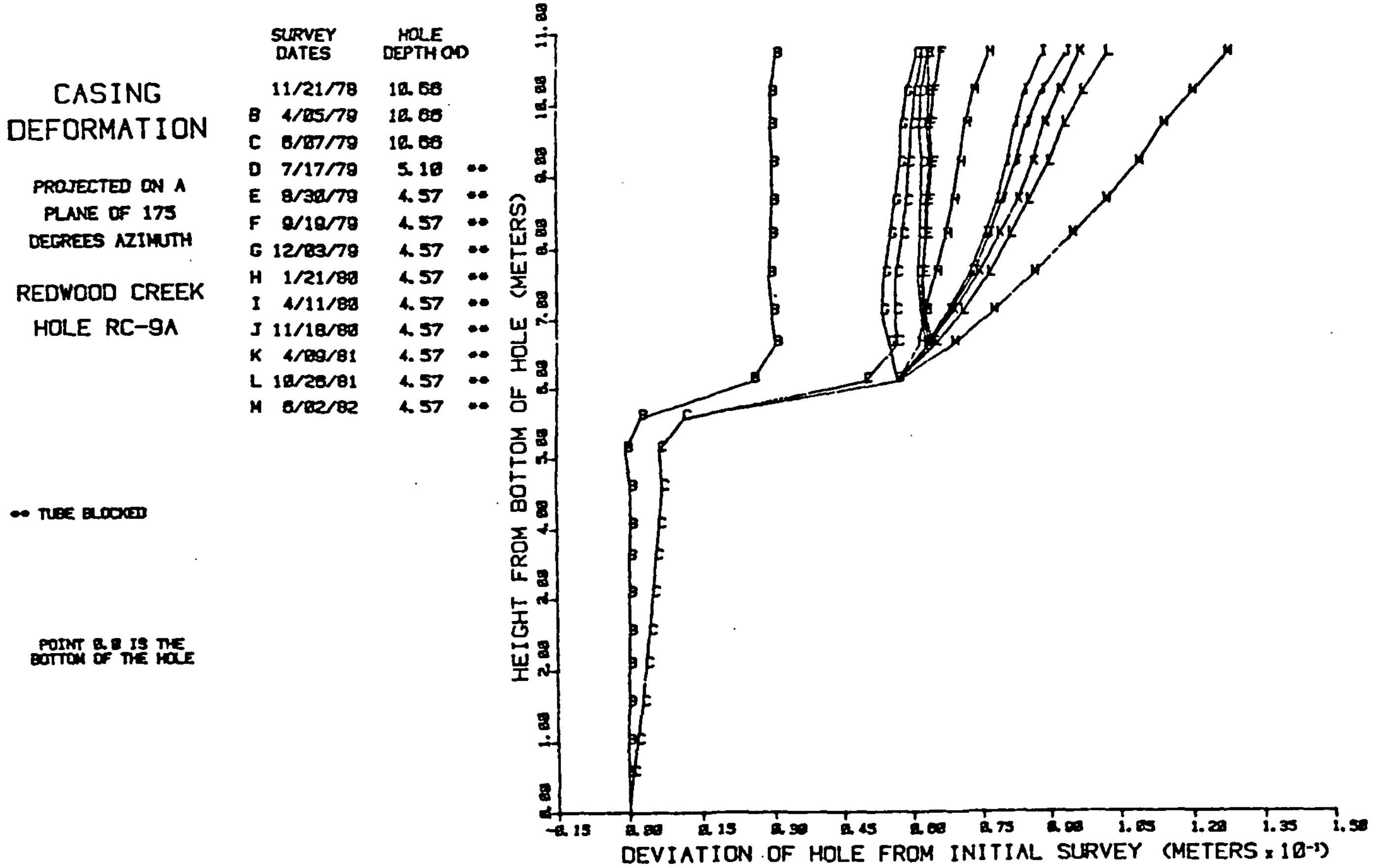

Figure 3. Representative inclinometer plot showing the base of the shear zone at 5.1 meters beneath the surface. This hole (RC-9A) is located in the central portion of the active area (see location map). The tube was installed in November 1978 and was blocked by movement in July 1979, indicated by the ** (courtesy of R. Ziemer, Redwood Sciences Laboratory, U.S. Forest Service, Arcata, CA).

average displacement of about 6 to 10 cmyr^{-1} at 4 m depth. Figure 3 is a typical plot of a 10.7 m deep inclinometer tube with the base of the shear zone at about 5.1 m beneath the surface. Note how narrow the shear zone appears to be on the inclinometer data.

METHODS

Seismic refraction is a standard geophysical exploration technique used to locate seismic velocity boundaries. Seismic boundaries result from either changes in the physical properties or composition of the material through which the seismic waves propagate. The seismic refraction technique is described in detail by numerous texts (e.g. Dobrin, 1976; Sheriff and Geldart, 1982; Kearey and Brooks, 1984). Seismic waves are generated at or near the surface by either mechanical means or the use of explosives. A linear array of vibration sensors, geophones, on the surface detects the arrival of the disturbance at preselected survey points. The seismograph serves as a relatively sophisticated time-measuring device which allows the determination of the travel time of the seismic wave from the source to each of the sensors. Travel time data is obtained for a source at each end, forward and reverse, of the array. A plot of travel time versus distance is used to calculate the velocity and depth of layer boundaries.

Shallow refraction investigations are subject to several inherent problems due to the nature of unconsolidated deposits and the relatively small magnitudes of the times and distances measured (Domzalski, 1956; Hagedoorn, 1959). Domzalski emphasized that one of the most significant problems is the uncertainty introduced by horizontal and vertical variation in the velocity of the overburden along a seismic line, which may be exaggerated in the case of landslide deposits. Some previous refraction landslide studies (e.g. Kobayashi, 1981; Trantina; 1962) have failed to use a sufficiently small geophone spacing in order to ensure that all velocity zones are identified. Possibly for these reasons there are few published earthflow refraction studies, although Cooksley (1964) examined an earthflow-type landslide in the Eel River basin using a single channel instrument.

In this study, seismic lines were run both parallel and transverse to the slope near the head and at midslope in the active portion of the landslide, and on the flanks adjacent to the active area (Figure 2, 4). Nine seismic lines of about 75 m length each were run using a Geometrics ES-1210 12-Channel Signal Enhancement Seismograph with an explosive source of 1/4 to 1 lb charges of 60 percent dynamite.

Each seismic line consisted of a linear array of 9 to 12 geophones with 6.1 m (20 ft) spacing between geophones. Shot locations were offset 6.1 m from the end of each array, resulting in a total line length of about 75 m (240 ft). The elevation of each geophone and shotpoint was surveyed. The spacing of geophones in this array did not allow determination of the near surface layer velocities. Consequently, a single channel Geometrics ES-125 Signal Enhancement Seismograph, with a hammer and strike plate source, was used to obtain direct arrivals from the surface layer and refracted arrivals from the layer just below it.

An elevation and weathering correction was initially applied to the raw travel time data to reduce the shots and geophones to a reference datum. The time of travel of the seismic wave through the material above the datum was subtracted from the first arrival time of the compressional wave at each geophone (Dobrin, 1976). This removes changes in travel time that are due to surface topography and the weathered surface material. It is then assumed that variation in the resulting corrected travel times is due to topography of the lower layer. In this study, the datum elevation was placed below the surface layer, reducing the analysis from a

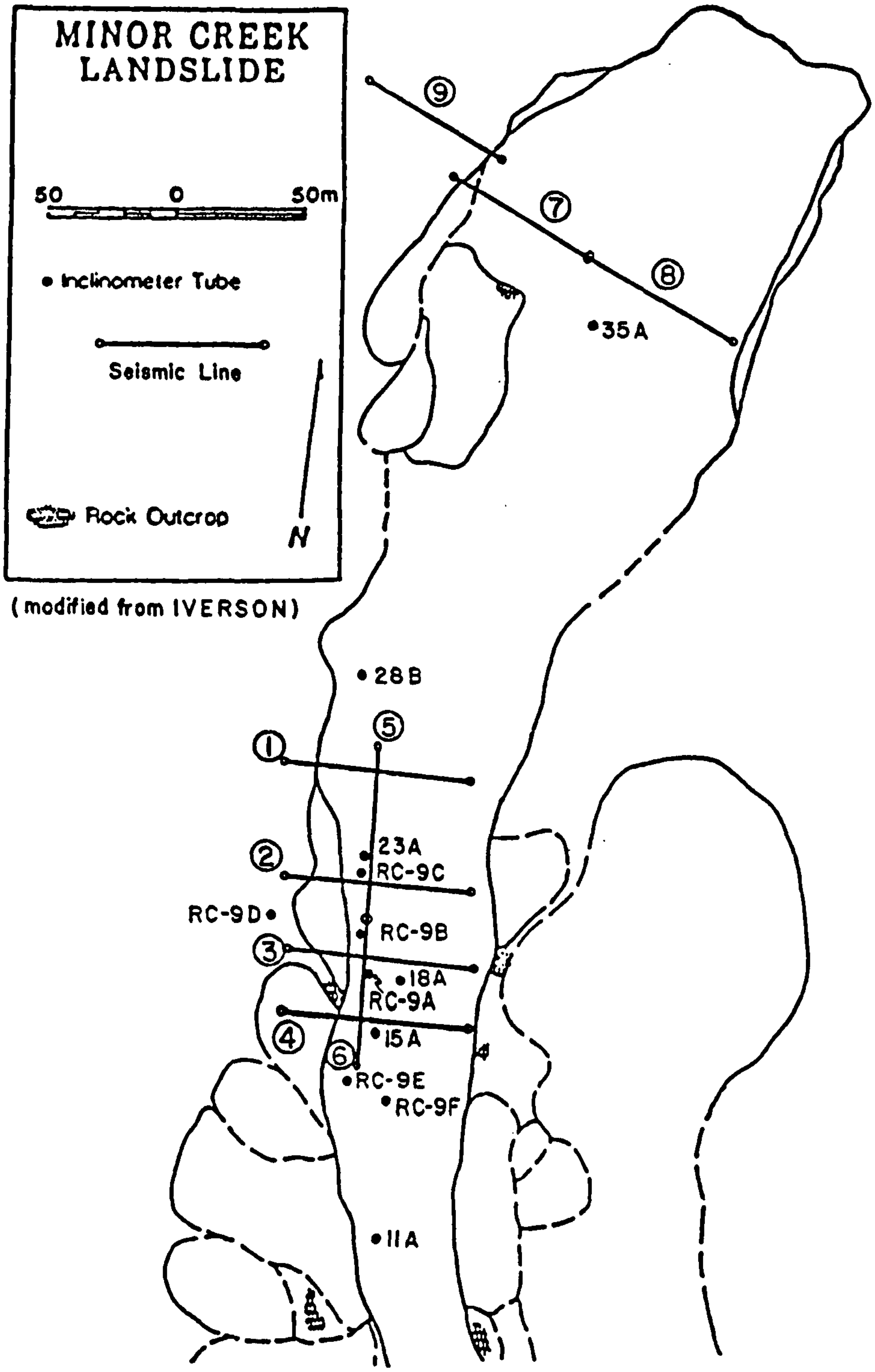

Figure 4. Plan view of seismic line and inclinometer tube locations. Circled endpoints of 12-channel lines indicate blast hole locations. Inclinometer tube sites are identified by solid dots and are labeled e.g., (RC-9D).

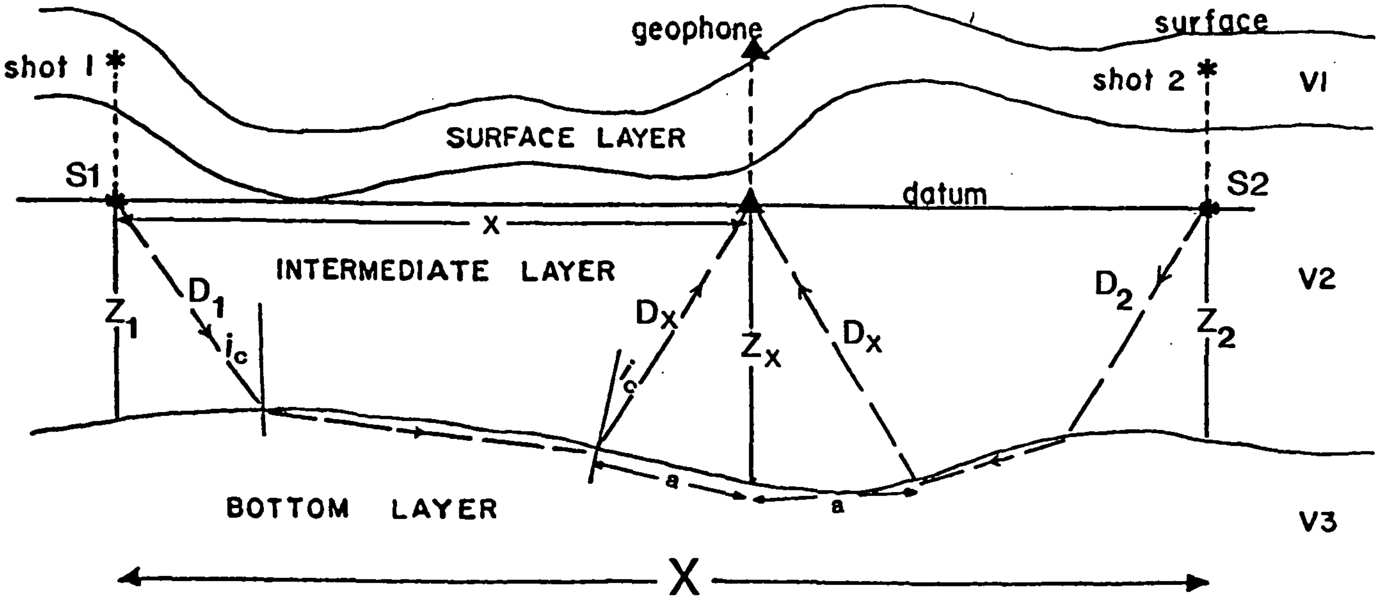

Figure 5. Schematic for delay-time analysis representing the field conditions encountered. Hypothetical ray paths for the three-layer case with irregular interfaces reduced to two-layer case after elevation correction applied. S, Z, and D refer to the shot, vertical distance, and raypath lengths, respectively. i_c is the critical angle. Dashed lines are the raypaths, with the arrows indicating propagation direction.

three- to two-layer problem (Figure 5).

Undulations in the refractor surface can be determined if the relief on the refractor is small in amplitude compared to average refractor depth, and the seismic line is long enough to obtain both forward and reverse travel times from the same refractor (Hagedoorn, 1959) (Figure 5). The Hagedoorn method assumes homogeneous, isotropic media, and uses the difference in travel times of compressional waves to an arbitrary geophone from both endpoints located a distance x from Source 1, S1, to determine the depth Z_x. The travel time t_1 from S1 to P and t_2 from Source 2, S2, to P are given by

$$t_1 = x/V3 + D_1 + D_x \tag{1}$$

$$t_2 = (X - x)/V3 + D_2 + D_x \tag{2}$$

where $V3$ is the seismic velocity in the bottom layer, X is the distance from shotpoint to shotpoint, and D_1, D_2 the time of travel to the boundary below the shotpoints. An important assumption is that the delay time D_x is the same in both directions, which requires undulations in the refractor to be small in order for this analysis method to be accurate.

The depth to the interface below each geophone is given by

$$Z_x = 0.5(t_1 + t_2 - t_{12})(V3 * V2)/(V3 - V2) \tag{3}$$

where V2 is the seismic velocity in the intermediate layer and t_{12} is the total travel time from S1 to S2.

The velocity of the layers was determined using both standard time-distance plot techniques (Dobrin, 1976) and the Hagedoorn "Minus" Method (Hagedoorn, 1959), the latter exclusively for the deepest boundary. In the "Minus" method, one-half the difference in travel times at each geophone for arrivals from S1 and S2 are plotted versus distance (Figure 6). The inverse of a least squares regression

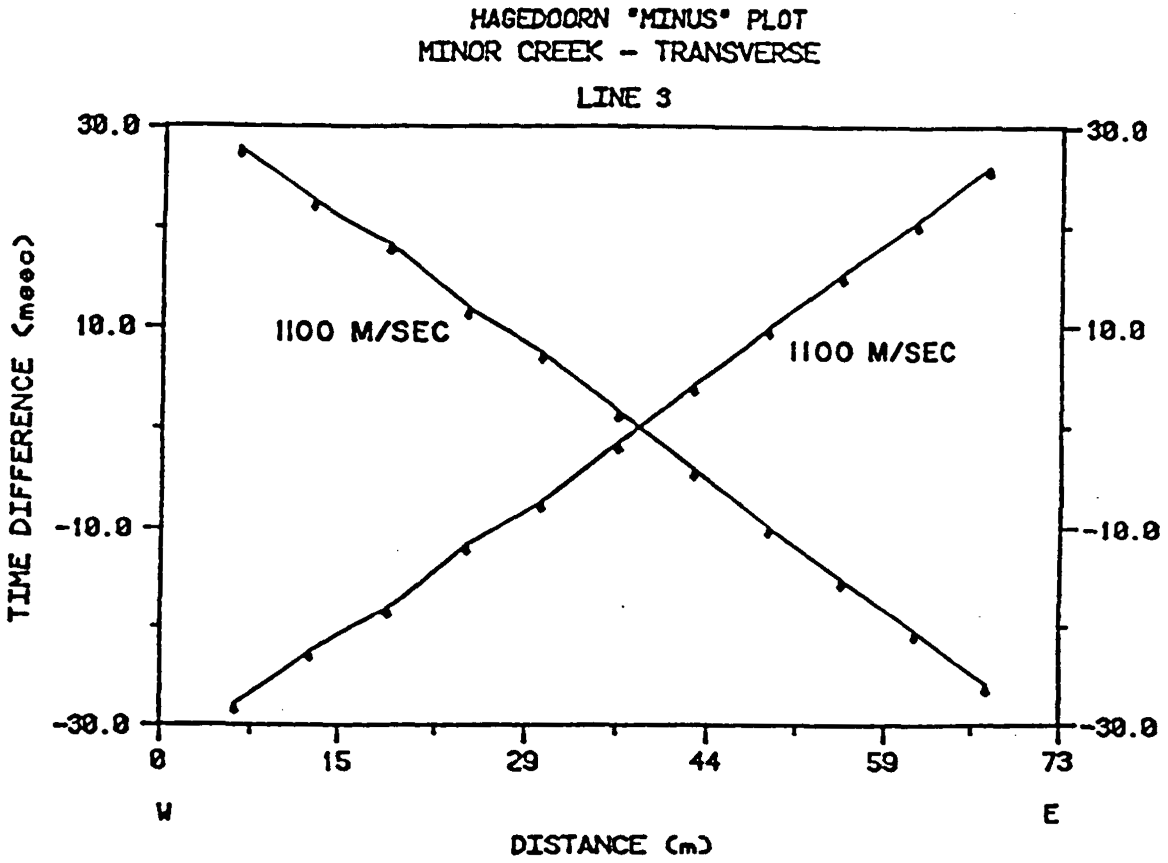

Figure 6a. Hagedoorn "minus" plot for Line 3. Velocities shown are the inverse of the least squares slope of the line.

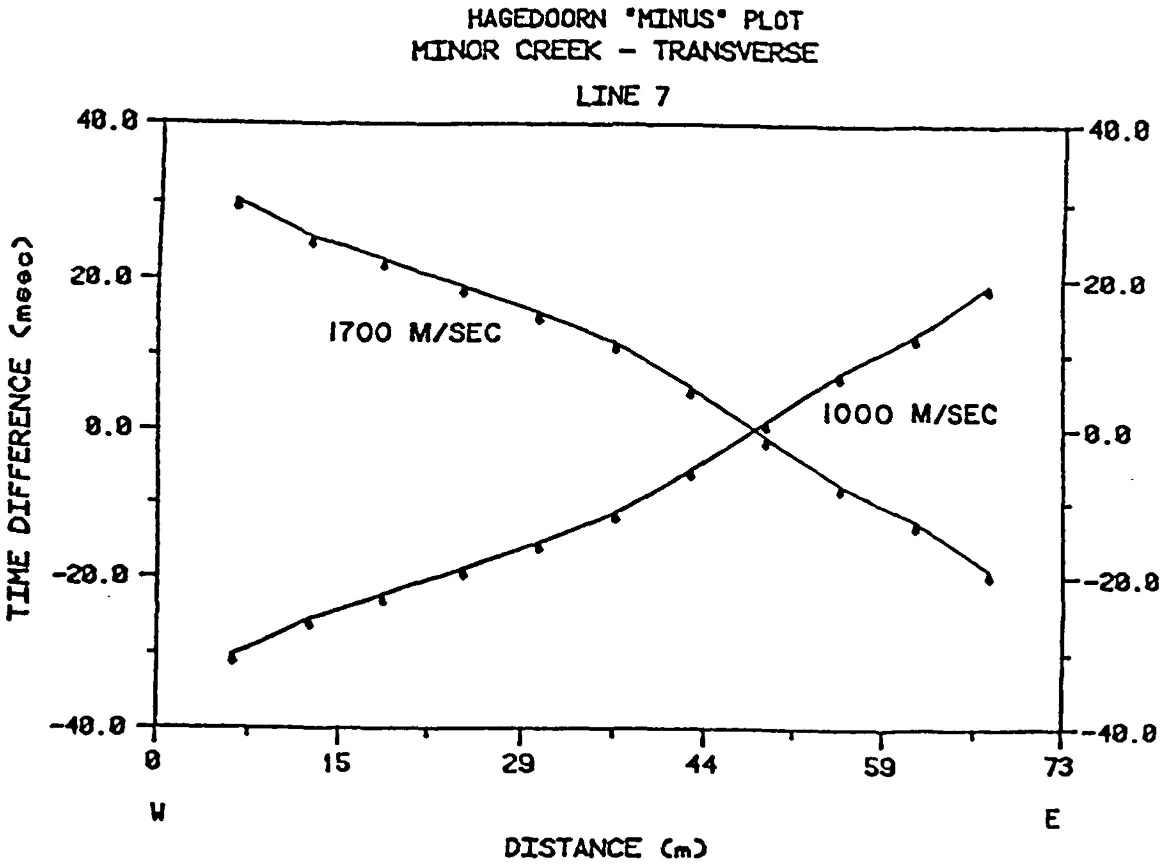

Figure 6b. Hagedoorn "minus" plot for Line 7. Velocities shown are the inverse of the least squares slope of the line. Note the distinct break in slope near the center of Line 7. This indicates that the velocity at the interface increases toward the west end.

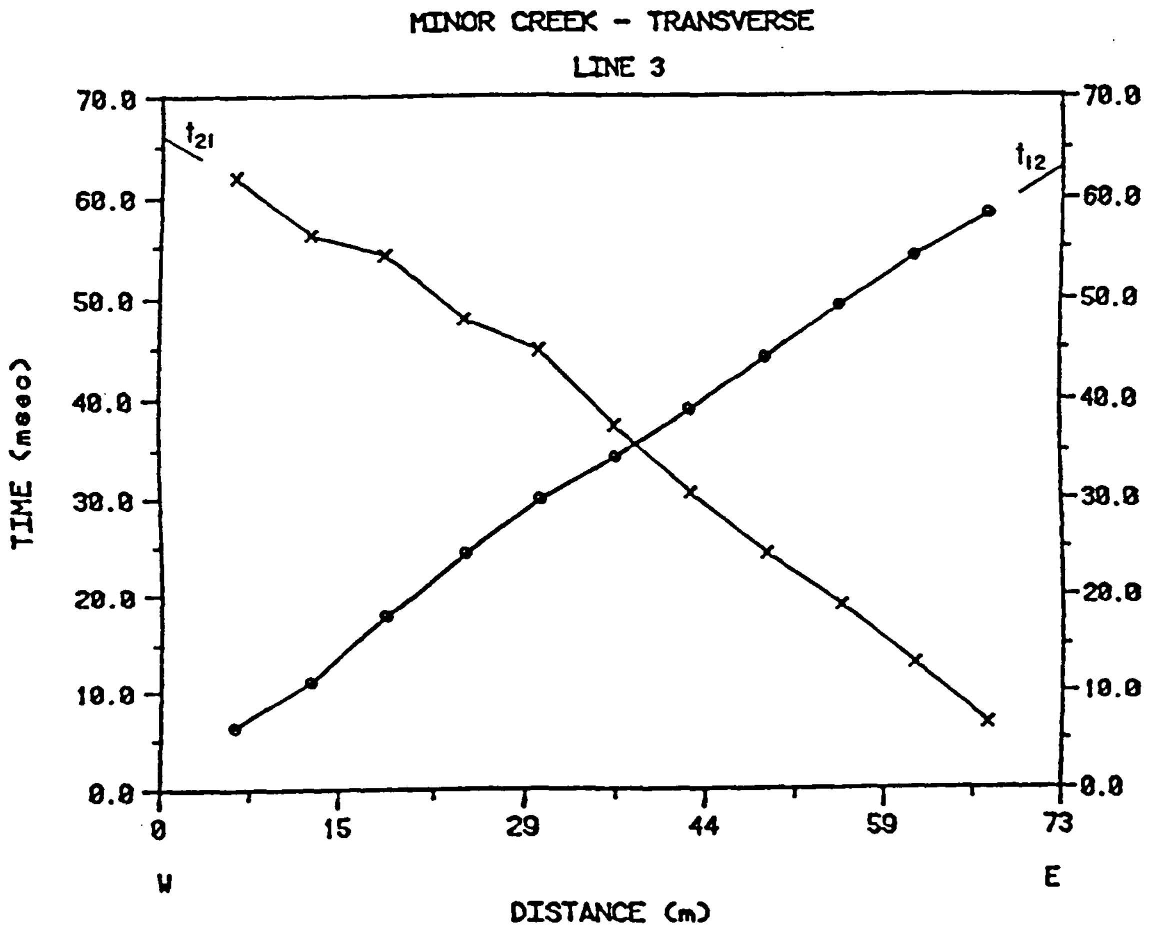

Figure 7. Time-distance plot of reduced travel time data for Line 3. Data points are shown for shots in both the forward and reverse directions: t_{12} and t_{21} are the total travel times in the forward and reverse directions, respectively.

fit of the Minus values gives the velocity. A roughly linear plot implies no lateral velocity variation within the layer. Figure 6a is an example of a constant layer velocity, while Figure 6b shows lateral variation which is identified by two roughly linear segments of different slope.

The time-distance plot of corrected travel times of each geophone versus distance from source (Figure 7) was used to determine the total travel time t_{12}. This should be approximately the same in both directions. Equation (3) could then be effectively applied to determine the depth to the lower boundary below each geophone. These point depths and the other layer boundaries were then plotted using rational cubic spline interpolation between data points.

RESULTS AND DISCUSSION

A three layer structure was consistently found throughout the earthflow. Results of the single channel instrument consistently showed a 1.5 to 2.5 m thick surface layer of 235 to 335 msec^{-1} velocity in all areas studied (Table I). This is typical of unconsolidated and uncompacted material (Clark, 1966; Redpath, 1973) and may represent the depth of maximum dessication. The base of this surface layer seems to agree with summer water table elevation which lies 1.5 to 2 m below the surface at various locations in the landslide (Iverson and Major, in preparation).

An intermediate velocity zone underlies the surface layer in all areas studied. The velocity in this layer varied from 630 to 720 msec^{-1} in the active portion of the earthflow, with higher velocities of 1050 to 1150 msec^{-1} consistently observed beneath stable appearing areas on the flanks of the earthflow. The lowest intermediate velocities are found beneath the most broken, active appearing surface terrain where inclinometer and stake like data show the greatest displacement (Iverson,

Table I. Average velocities ($msec^{-1}$) for each layer and minimum and maximum depths (m) for seismic Lines 1 to 9.

Line No.	V1	V2	V3	Z_{min}	Z_{max}
	—	— msec^{-1} —	—	— m	—
1	290	700	1215	3.8	7.4
2	255	700	1130	4.7	9.2
3	269	720	1125	4.6	8.8
4	255	655	1280	4.8	10.4
5	335	700	1130	5.9	11.5
6	290	700	1180	5.4	9.5
7	235	630	1340	3.4	6.3
8	235	630	1020	5.4	9.1
9	290	1070	1070	3.9	8.7

1984). This suggests that the more active areas have experienced greater disruption with the lower velocities related to an increase in bulk porosity. The depth to the base of the intermediate layer was determined with the 12 channel instrument. The depths to the deepest boundary varied between 3.5 to 11.5 m (Figures 8 and 9). Depths of intersecting points from transverse and longitudinal lines showed good agreement. The velocity of this deepest boundary ranged from about 1000 to 2100 $msec^{-1}$ (Table I). The typical velocity of about 1130 $msec^{-1}$ is well below that of competent Franciscan bedrock, generally above 5000 $msec^{-1}$ (Stewart and Peselnick, 1977), and is within the range of 900 to 1500 $msec^{-1}$ determined by Cooksley (1964) for weathered, sheared, and fractured regolith derived from Franciscan bedrock in the Eel River basin (see Figure 1). This implies that failure is occurring within the clay-rich matrix material.

Cooksley's results show a weighted mean velocity of about 2100 $msec^{-1}$ for weathered Franciscan bedrock, which matches the highest velocity observed which is found below Line 9. Although there is considerable variation in the lithology of Franciscan rocks (reference), these results suggest that the flanks are supported by more competent material that may be connected to bedrock.

The velocity of the deepest layer detected beneath Line 8 and the east half of Line 7 is close to the intermediate velocity of Line 9. The western half of the Hagedoorn Minus plot for Line 7 (Figure 6b) shows a distinct velocity increase to about 1700 $msec^{-1}$, approaching that of the deepest boundary at Line 9. The common velocity of about 1100 $msec^{-1}$ for the intermediate zone beneath the flanks and the deepest boundary beneath the active portions of the earthflow suggests they may be the same material. The lower intermediate zone velocity in the active portion may be the result of disruption of the 1100 $msec^{-1}$ material. Shots offset about 60 m (200 ft) from the endpoints of Line 8, for an effective line length of

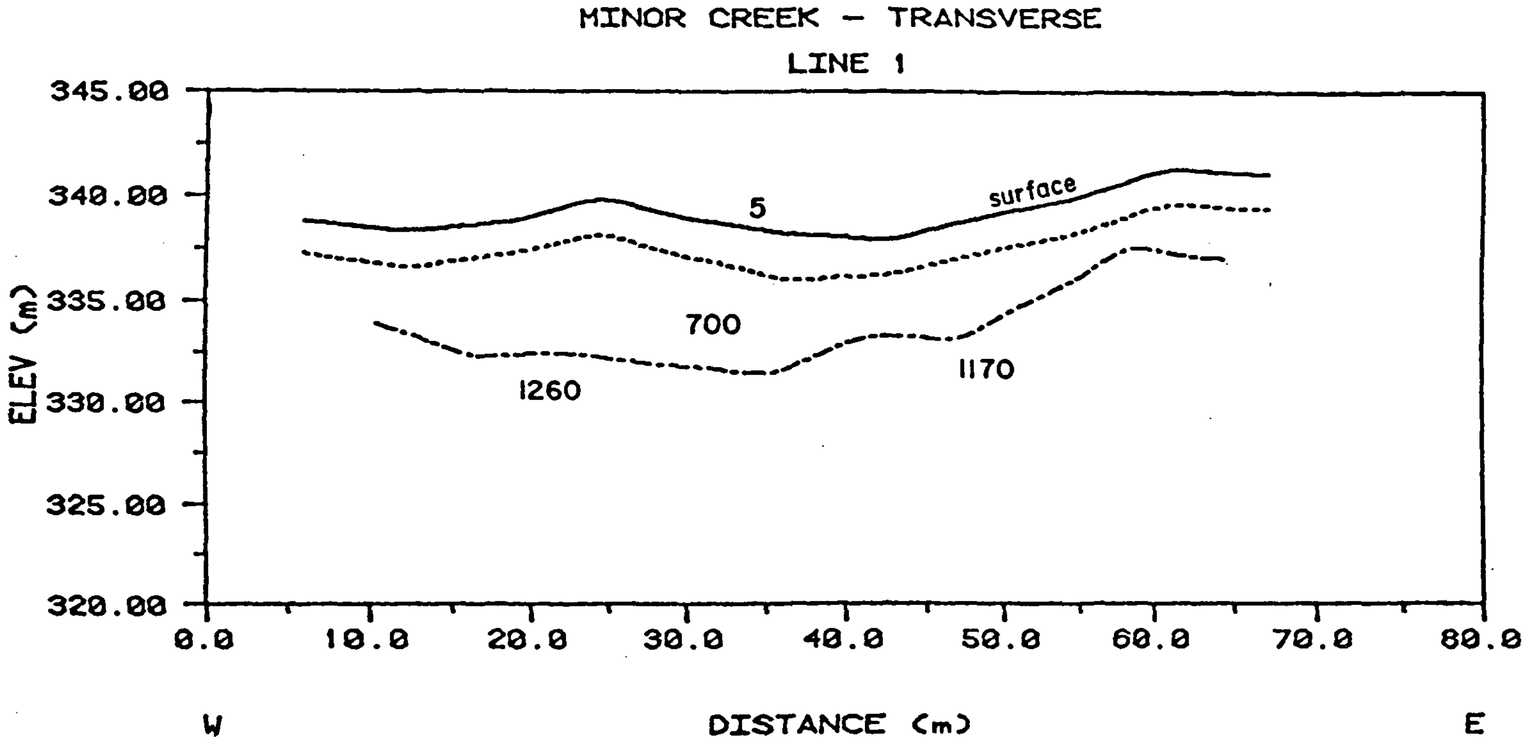

Figure 8a. Cross-section plot of seismic results for transverse Line 1. Velocities in msec^{-1} for the bottom layer at the forward (0.0 end) and reverse ends, and the intermediate layer, are shown. The number on the surface indicates the location of the intersection of Line 1 with longitudinal seismic Line 5.

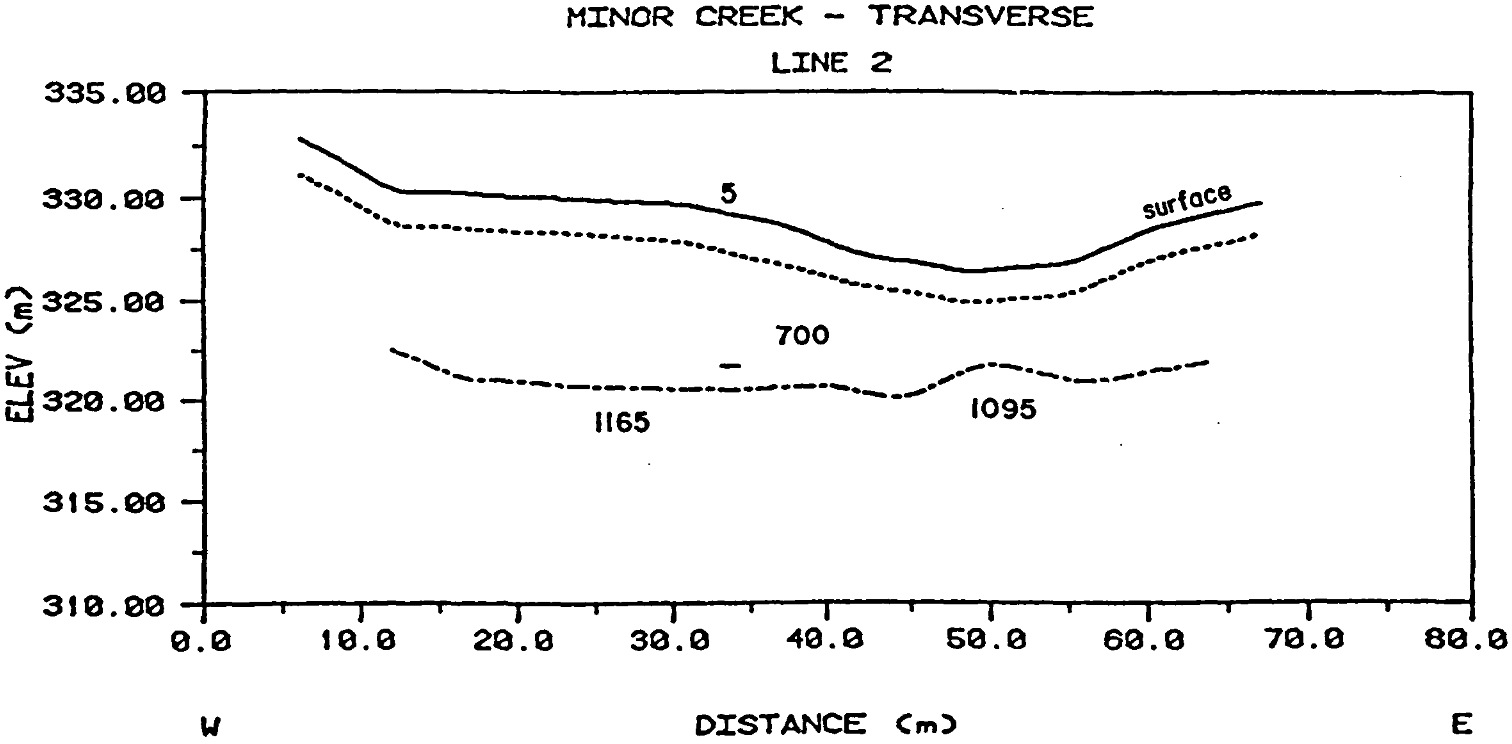

Figure 8b. Cross-section plot of seismic results for transverse Line 2. Velocities in $msec^{-1}$ for the bottom layer at the forward (0.0 end) and reverse ends, and the intermediate layer, are shown. The number on the surface indicates the location of the intersection of Line 2 with longitudinal seismic Line 5, with horizontal bar below the number representing the depth to the bottom boundary for that line.

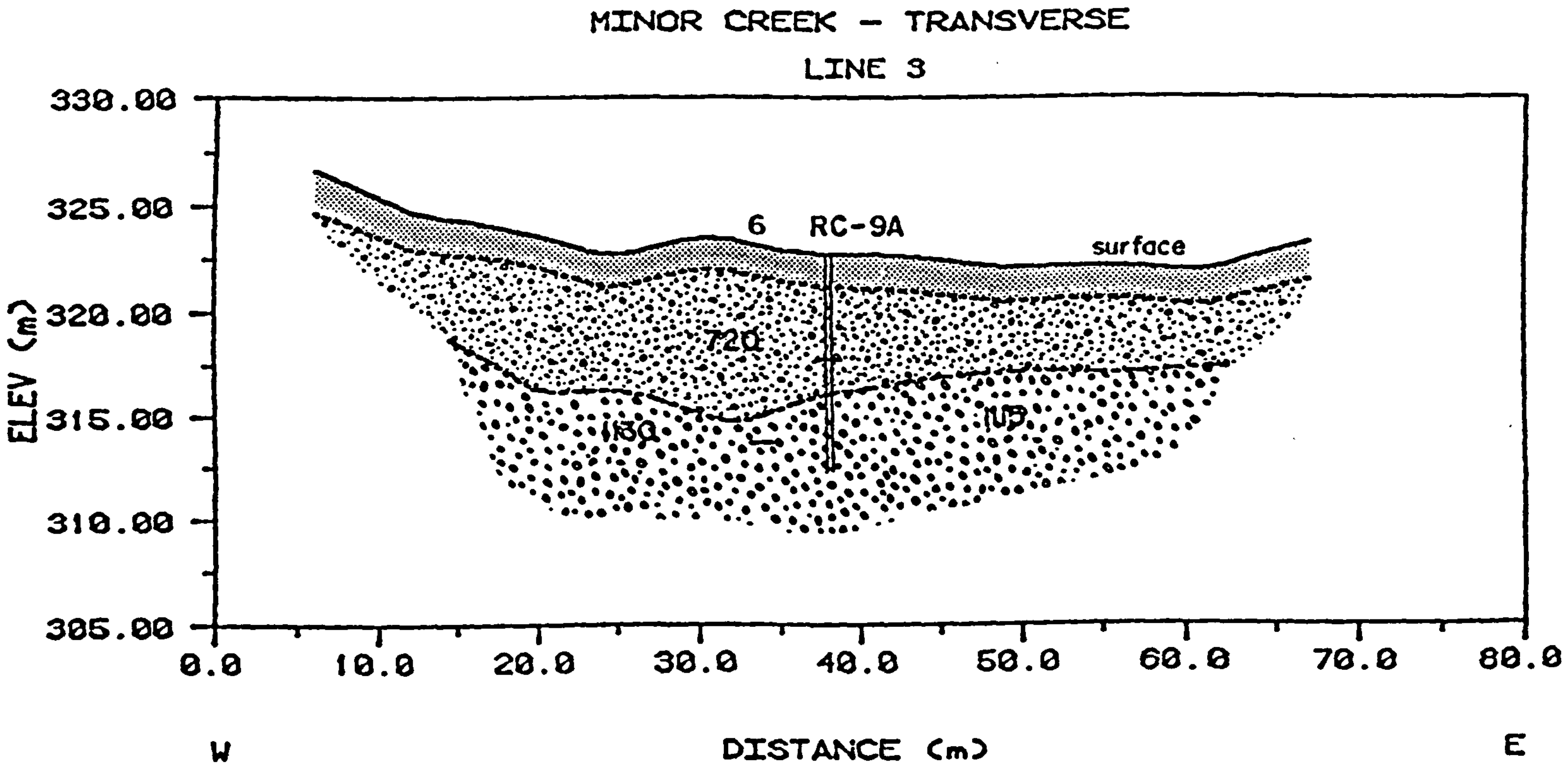

Figure 8c. Cross-section plot of seismic results for transverse Line 3. Velocities in $msec^{-1}$ for the bottom layer at the forward (0.0 end) and reverse ends, and the intermediate layer, are shown. Also shown is the location and depth of nearby inclinometer tube RC-9A, with the horizontal line cutting the tube indicating the base of the shear zone determined by that method. The number on the surface indicates the location of the intersection of Line 3 with longitudinal seismic Line 6, with horizontal bar below the number representing the depth to the bottom boundary for that line.

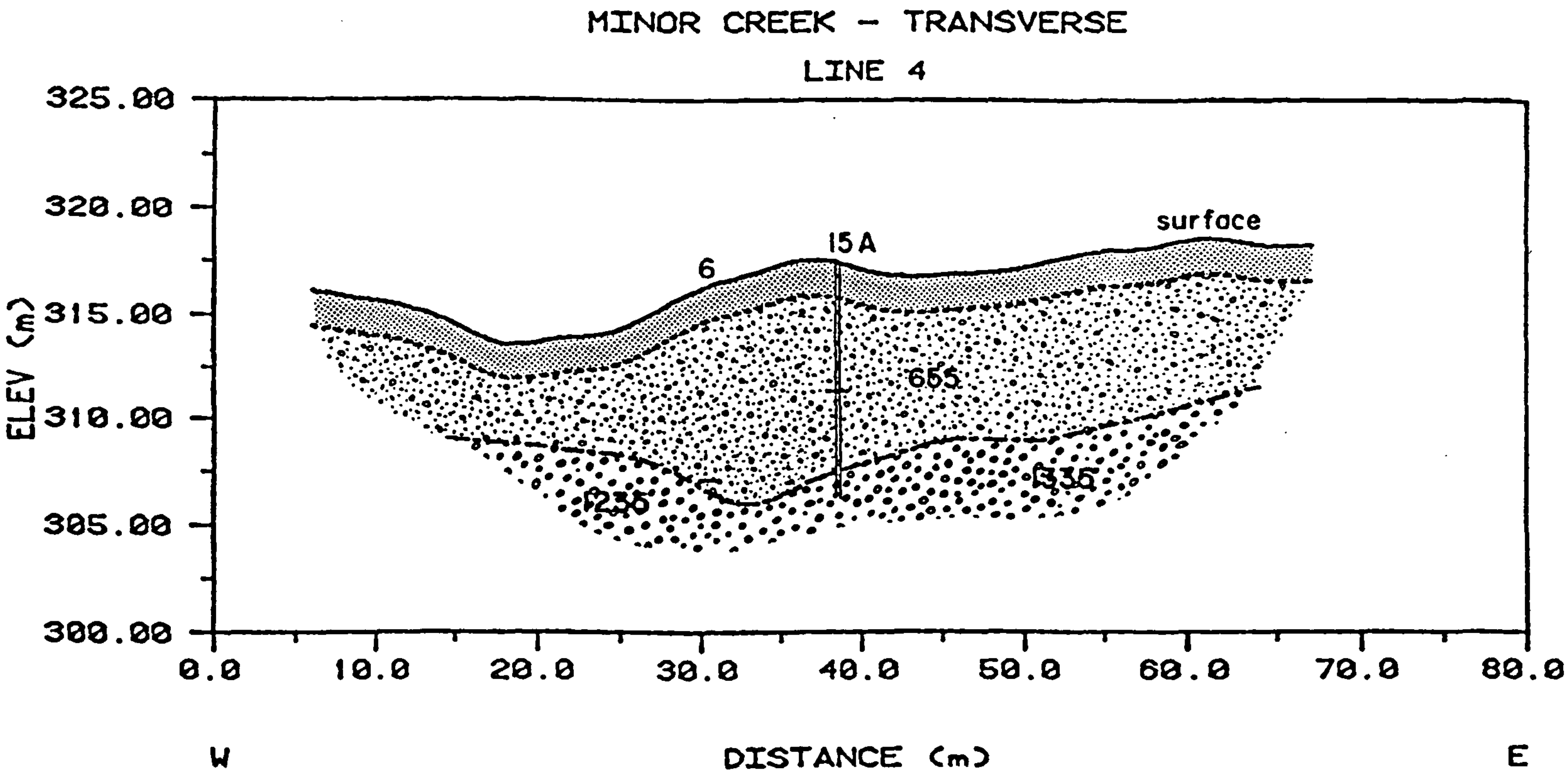

Figure 8d. Cross-section plot of seismic results for transverse Line 4. Velocities in msec^{-1} for the bottom layer at the forward (0.0 end) and reverse ends, and the intermediate layer, are shown. Also shown is the location and depth of nearby inclinometer tube 15A, with the horizontal line cutting the tube indicating the base of the shear zone determined by that method. The number on the surface indicates the location of the intersection of Line 4 with longitudinal seismic Line 6, with horizontal bar below the number representing the depth to the bottom boundary for that line.

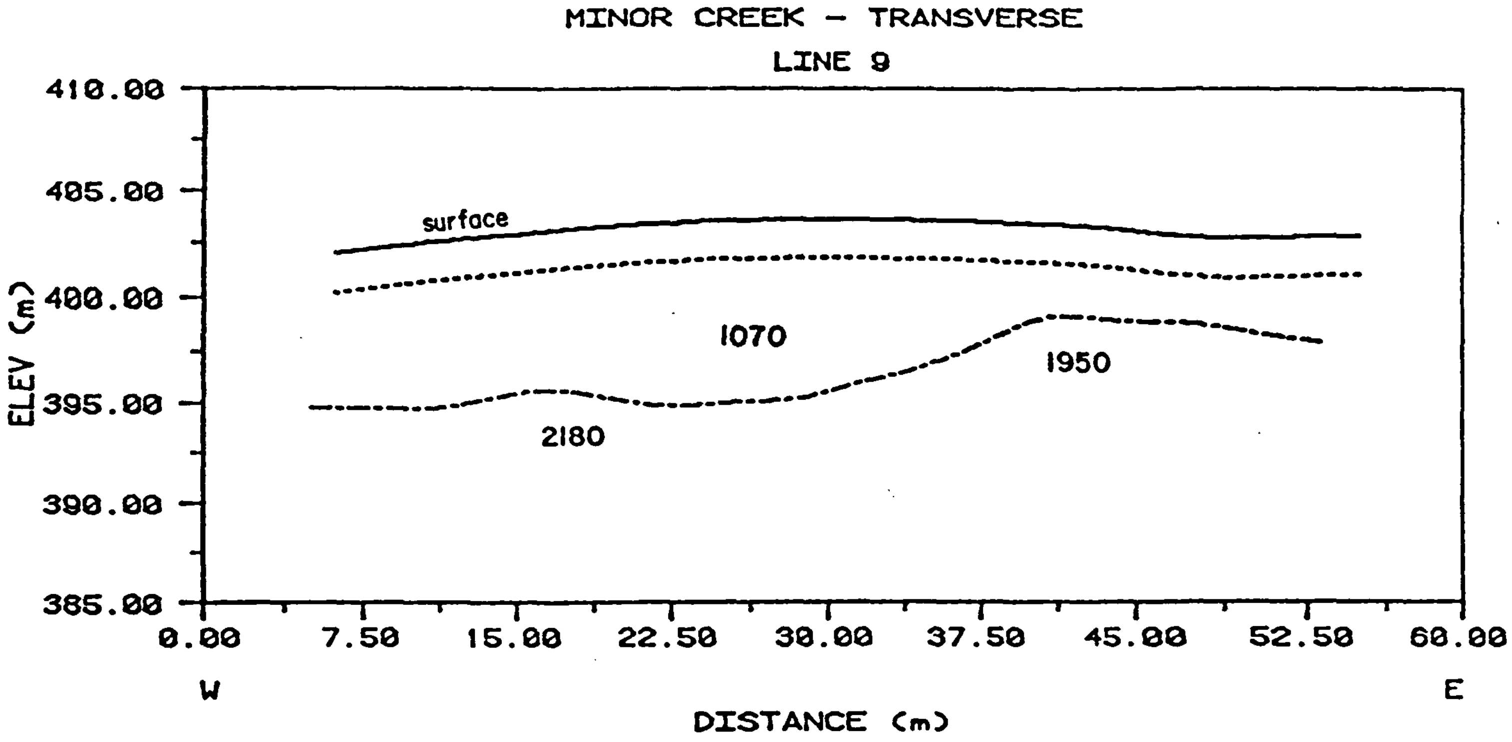

Figure 8e. Cross-section plot of seismic results for transverse Line 9. Velocities in msec^{-1} for the bottom layer at the forward (0.0 end) and reverse ends, and the intermediate layer, are shown.

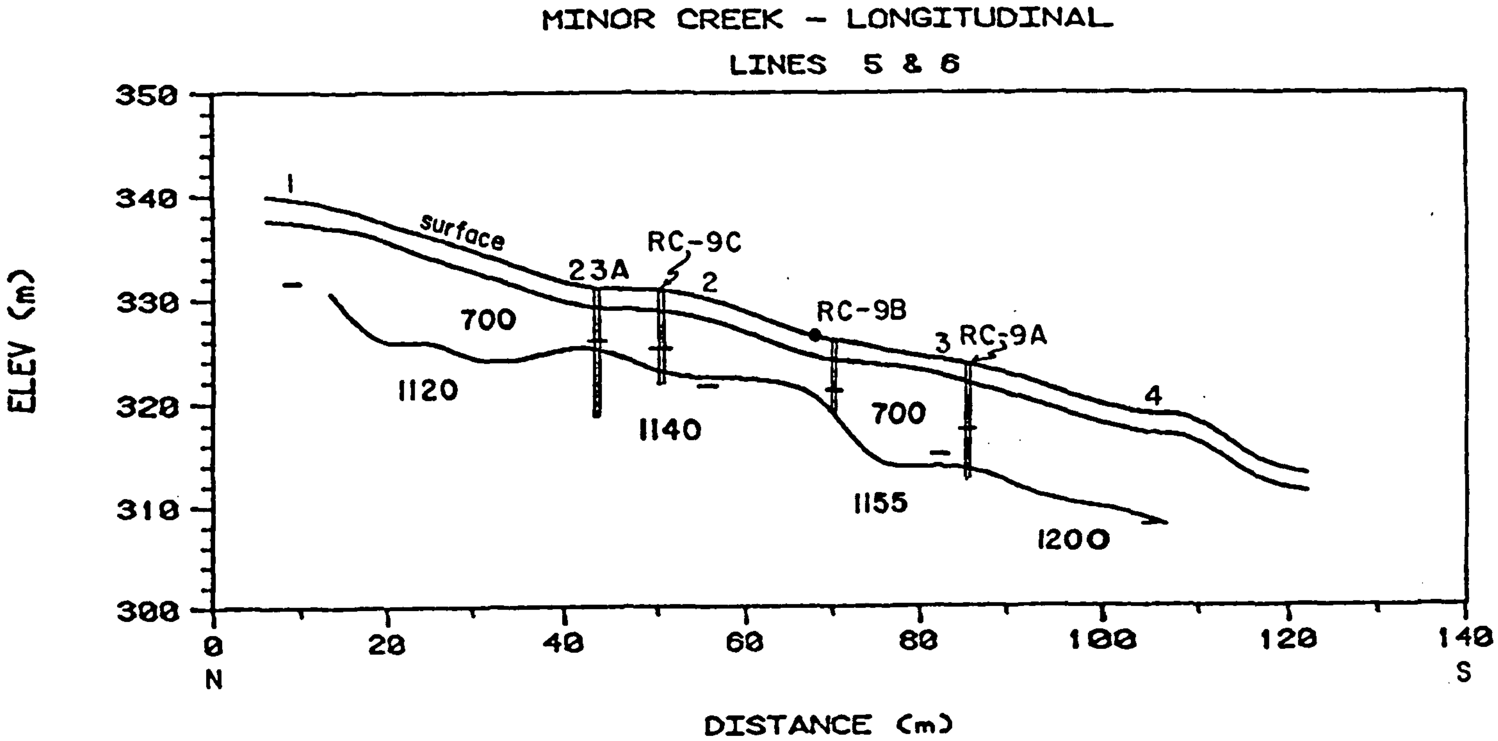

Figure 9a. Combined cross-section plot of seismic results for Lines 5 & 6. Velocities in msec^{-1} for the bottom layer and the intermediate layer are shown. Numbers on the surface indicate the location of intersection with other seismic lines, with horizontal bars below the numbers the respective depths determined at that point. Nearby inclinometer tubes are indicated by parallel vertical lines with their respective shear zone depths indicated by horizontal lines cutting the tubes. The solid circle on the surface is the common endpoint.

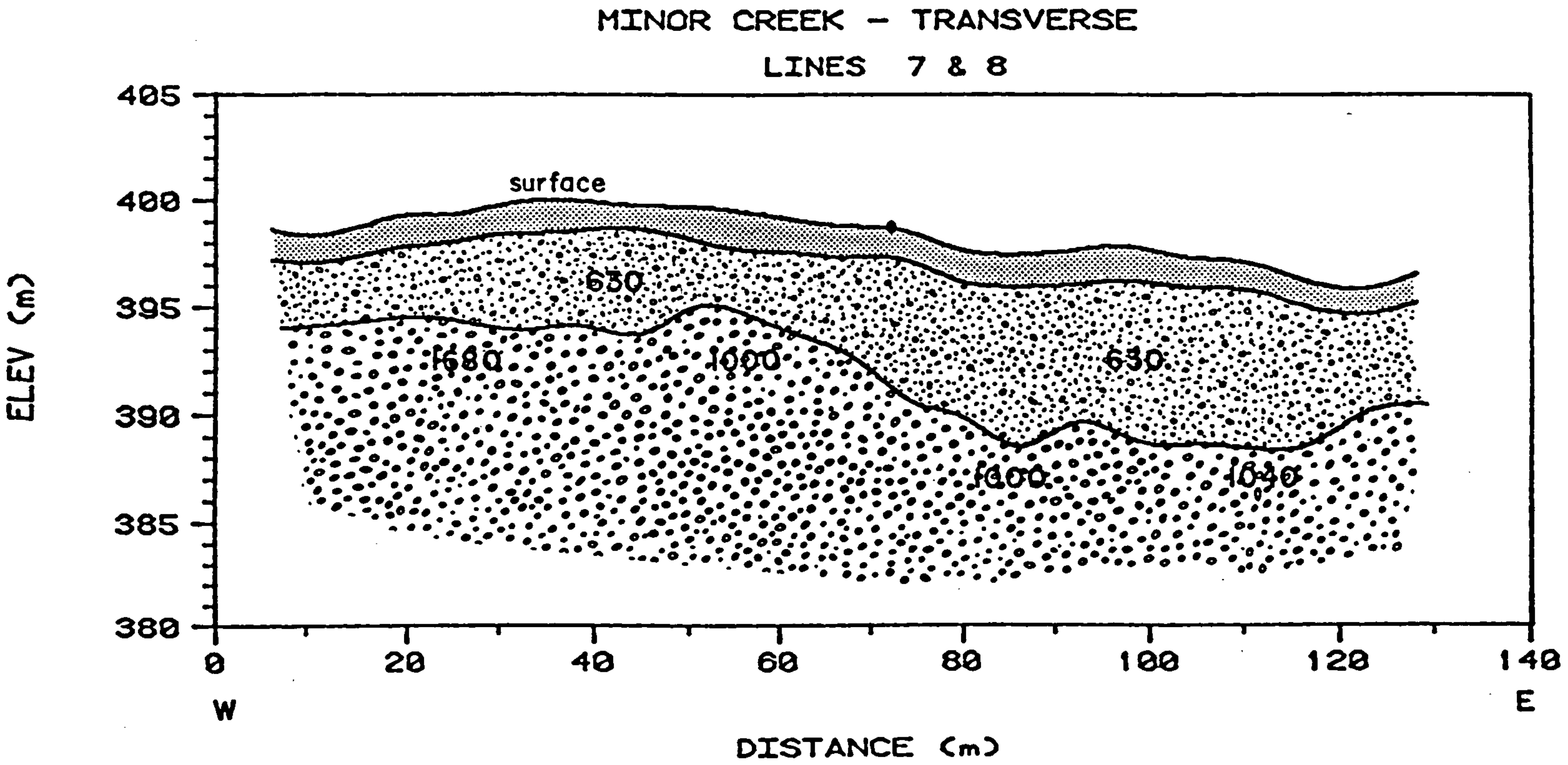

Figure 9b. Combined cross-section plot of seismic results for Lines 5 & 6. Velocities in msec^{-1} for the bottom layer and intermediate layers are shown. The solid circle on the surface is the common endpoint.

about 180 m (600 ft), did not detect the 2100 msec^{-1} material beneath the active portion of the earthflow. These data suggest that failure is occuring within areas where either the 1100 msec^{-1} material has a considerably greater thickness than on the flanks, or the more competent 2100 msec^{-1} underlying support material is absent.

The generalized cross-section of the results for Lines 7, 8, and 9 is presented in Figure 10. Single channel results for a 19 m line on the flank west of Line 4 (Figure 4) indicate the presence of the 2100 msec^{-1} material at a depth of about 6.5 m. This higher velocity material was not detected beneath Lines 1 to 6, and it could not be determined from the data available whether the 2100 msec^{-1} material underlies any of the active areas at depth. However, the above findings intimate that the location of the active portion of the Minor Creek landslide is structurally controlled.

COMPARISON OF SEISMIC AND INCLINOMETER DATA

Iverson (1984) concluded from inclinometer data that the base of the shear zone averages 5 to 8 m beneath the active portion of the landslide, and is somewhat thicker near its longitudinal axis. This trend is in general agreement with seismic results (Figures 8,9), although the seismic interface is generally about 1 m deeper than the inclinometer break.

Inclinometer tubes located near seismic lines are plotted in Figure 8 and 9. Horizontal lines on the tubes indicate the depth of the base of the shear zone. Both inclinometer and seismic evidence indicate that the depth of this boundary varies by as much as 5 m over horizontal distances of about 10 m. This could explain some of the difference in results for inclinometers located a few meters from seismic lines. The differences can also be attributed in part to uncertainties in the seismic data

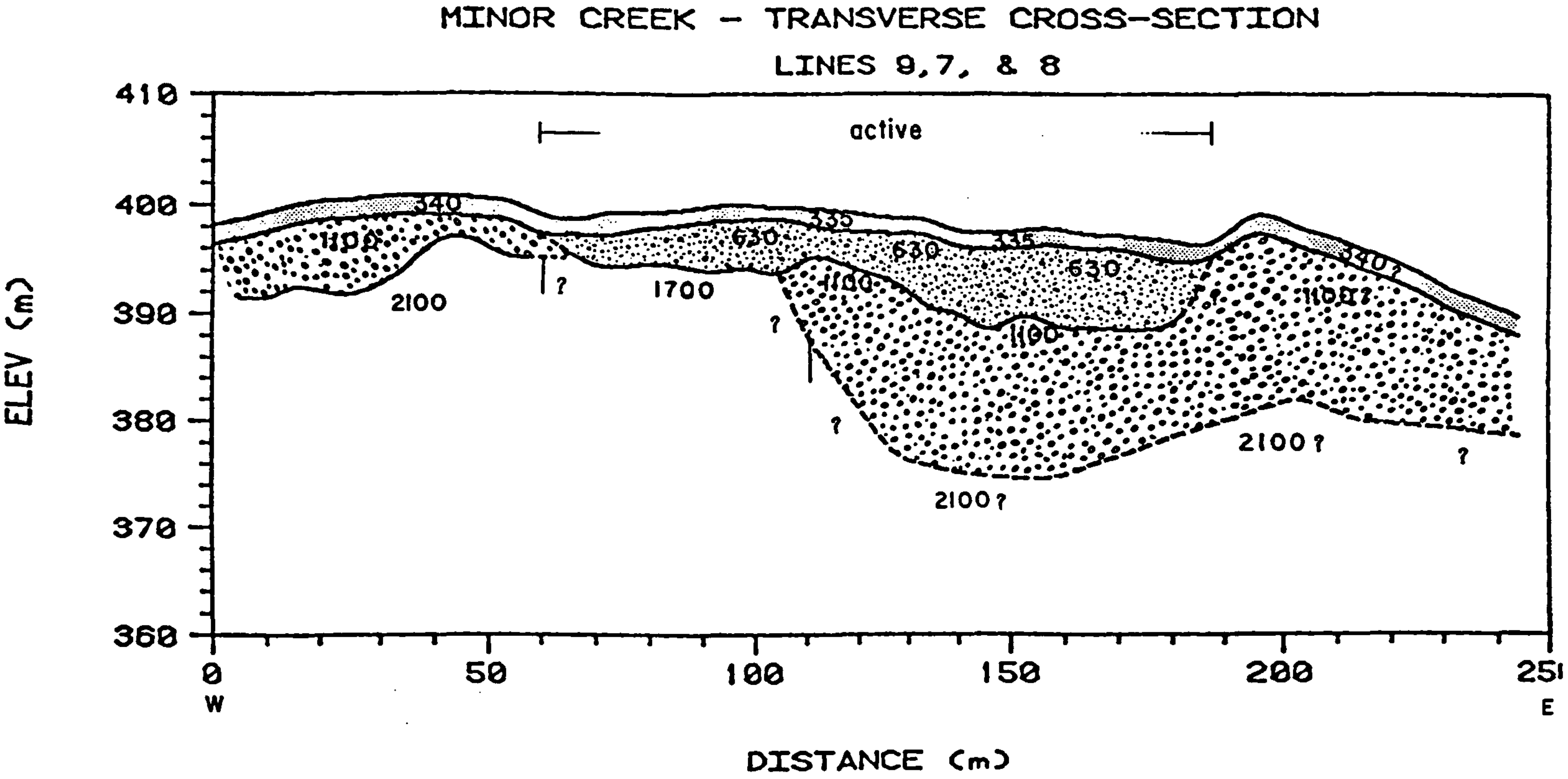

Figure 10. Generalized cross-section based on Lines 7, 8, and 9. Solid lines are approximate boundaries determined from seismic data. Dashed lines suggest possible continuation of these boundaries. Velocities in msec^{-1} for the bottom layer and intermediate layers are shown. Vertical bars indicate the location of possible velocity transition zones. Question marks indicate an inferred boundary or velocity.

analysis and a possible 5 percent discrepancy due to survey error. Zones or lenses of low velocity material within the intermediate layer may also provide a significant contribution to overestimation of the depth.

SUGGESTED FURTHER STUDY

Recently collected data with the single channel instrument at the Minor Creek site shows a greater variation in the surface layer velocity than was previously determined (Bromirski and Dengler, 1985). This was due to having mistakenly identified the air-coupled wave arrival as the compressional wave arrival at some locations (Knapp, 1986 or in preparation). However, this latest data was taken under considerably drier conditions than previous surface data or than conditions under which the 12-channel data was collected. A more detailed surface velocity study under various saturation conditions is therefore recommended. This may result in bringing the depths of the lower boundary more in accord with the base of the shear zone identified by Iverson (1984) from inclinometer data.

Additional information on the physical properties of the earthflow material can be obtained by examining the near surface layer compressional and shear wave velocities in greater detail. An estimate of the bulk and shear elastic moduli, and consequently Poisson's ratio, may be determined if shear wave velocities can be obtained for the near surface layer. More information on the degree of lateral variation in this layer would also be useful to more accurately map the deepest seismic interface.

CONCLUSION

A three layer structure was consistently found throughout the earthflow complex. Two seismic boundaries and four different velocity zones were identified. The shallow near surface boundary seems to be associated with water table depth. The more irregular lower boundary was generally about 1 m deeper than the base of the shear zone identified by Iverson from inclinometer data in the lower portion of the earthflow. The difference can be attributed in part to uncertainty in the analysis method, survey error, and/or the presence of zones or lenses of low velocity material within the intermediate layer. Inclinometer and seismic evidence indicate that the depth of the base of the shear zone varies considerably over small horizontal distances.

Significantly higher velocities for both the intermediate and deepest layer interfaces were found beneath the stable flanks, which appear to be underlain by a seismically faster and therefore more competent material. It could not be determined from the available data whether the highest velocity material identified underlies the active portion. The seismic results intimate that the location of the active portion of the Minor Creek earthflow is structurally controlled.

Similar velocities observed for the intermediate layer beneath the flanks and the deepest boundary in the active portion suggest they are the same material. The lower velocity of the intermediate layer in the active portion can be attributed to disruption of this material resulting in higher bulk porosity. The general agreement of the depth of the deepest boundary in the active portion with inclinometer results implies that the shear zone in earthflows is detectable using the refraction technique. The seismic results show this zone to be continuous throughout the earthflow.

ACKNOWLEDGEMENTS

This project was partially funded by McIntire-Stennis Research Grant No. 70 under the auspices of Dr. Carl Yee, Humboldt State University, Arcata, CA. Thanks to Jim Cooksley of Cooksley Geophysics, Redding, CA for generously loaning me the 12-channel instrument and giving me invaluable advise. Very special thanks to Dr. Lori Dengler of the H.S.U. Geology Department for her advice, support, field assistance, and constructive criticism. Bob Ziemer of the U. S. Forest Service Redwood Science Lab provided assistance with the inclinometer data and reviewed this paper.

Also thanks to Dick Iverson of the U.S.G.S. David A. Johnstone Cascades Volcanic Observatory for the generous use of his figures, and for providing the background study to which the seismic results were compared.

Finally, much appreciation for the many field assistants who helped with data collection and surveying, especially Mike Hollins and Charlie Watson who helped with the blasting for the 12-channel portion of the study

REFERENCES

Bromirski, P. D. 1985. 'Depth of channel alluvium estimated by seismic refraction profiling', In: *Proc. of the Humboldt Conference on Environmental Systems and Natural Resources, April 28, 1984*, R. Lamberson, ed., Humboldt State U., Arcata, CA, 52-70.

Bromirski, P. D. 1985. 'Seismic refraction investigation of an earthflow in Redwood Creel basin, northwestern California', *Transactions, Americ. Geophys. Union,* 66, p.889, abs.

Clark, S. P. 1966. *Handbook of Physical Constants, Revised Edition.* The Geological Society of America, Inc., New York, 587 pp.

Cooksley, J. W. 1964. 'Geological investigation of a landslide employing seismic exploration technique', In: *Engineering Geology and Soils Engineering Symposium, 2nd Ann., 1964, Proc.,*, Pocatello, Idaho, Idaho State University, Pocatello, Idaho, 97-103.

Dobrin, M. B. 1976. *Introduction to Geophysical Prospecting*, McGraw-Hill, Inc., New York, NY, 630 pp.

Domzalski, W. 1956. 'Some problems of shallow refraction investigations', *Geophys. Prospecting*, 4, 140-156.

Hagedoorn, J. G. 1959. 'The plus-minus method of interpreting seismic refraction sections', *Geophys. Prosp.*, 7, 158-182.

Harden, D. R., Janda, R. J., and Nolan, K. M. 1978. *Mass Movement and Storms in the Drainage Basin of Redwood Creek, Humboldt County, California - A Progress*

Report, U.S. Geological Survey Open-File Report 78-486, U. S. Government Printing Office, Washington, D. C., 161 pp.

Harden, D. R., Kelsey, H. M., Morrison, S. D. and Stephens, T. A., 1982. *Geologic map of the Redwood Creek drainage basin, Humboldt County, California, U. S. Geological Survey Water Resources Investigations Open-File Report* 81-496, U. S. Government Printing Office, Washington, D. C., 1 sheet.

Iverson, R. M. 1984. *Unsteady, Nonuniform Landslide Motion: Theory and Measurement*, Ph.D. dissertation, Stanford University, Palo Alto, CA, 303 pp.

Iverson, R. M. and Major, J. J. (in preparation). 'Detailed hydrogeology of a persistent landslide: patterns of groundwater flow and propensity for slope movement', (to be submitted to *Geol. Soc. Amer. Bull.*), U.S. Geological Survey, David A. Johnston Cascades Volcano Observatory, 5400 MacArthur Blvd., Vancouver, WA.

Janda, R. J, Nolan, K. M., Harden, D. R., and Colman, S. M. 1975. *Watershed Conditions in the Drainage Basin of Redwood Creek, Humboldt County, California, as of 1973, U. S. Geological Survey Open-File Report 75-568*, U. S. Government Printing Office, Washington, D. C., 266 pp.

Janda, R. J. 1979. 'Summary of regional geology in relation to geomorphic form and process', In: *A Guidebook for Field Trip to Observe Natural and Resource Man Agement- Related Erosion in Franciscan Terrain of Northwestern California*, Cordilleran Section of the Geological Society of America Annual Meeting, Geol. Soc. Am., Cordilleran Sect., Boulder, CO, II.1 - II.17.

Janda, R. J., Nolan, K. M., and Stephens, T. A. 1980. 'Styles and rates of landslide movement in slump-earthflow-sculpted terrain, northwestern California (Abstract)', *Geological Society of America 76th Annual Meeting Abstracts* *with Programs*, **12**, Geol. Soc. Am., Cordilleran Sect., Boulder, CO, 113.

Kearney, P. and Brooks, M. 1984. *An Introduction to Geophysical Exploration*, Blackwell Scientific Publications, Palo Alto, CA, 296 pp.

Keefer, D. K. and Johnson, A. M. 1983. Earthflows: morphology, mobilization and movement, *U. S. Geological Survey Professional Paper* **1264**, 56 pp.

Kelsey, H. M. 1977. *Landsliding, Channel Changes, Sediment Yield and Land Use in the Van Duzen River Basin, Northcoast California, 1941-1975*, Ph.D. dissertation, University of California, Santa Cruz, 302 pp.

Knapp, R. W. 1986. (in preparation). 'Observations of the air-coupled wave as a function of depth', (submitted to *Geophysics* Jan 1986), Kansas Geological Survey, University of Kansas, Lawrence, Kansas.

Kobayashi, Y. 1981. 'The seismic refraction survey in landslide areas', *Disaster Prevention Research Institute, Bulletin*, Kyoto Univ., **31**, Part 1, 275, 1-15.

Nolan, K. M. and Janda, R. J. (in preparation). 'Sediment discharge and movement of two earthflows in Franciscan terrain, northwestern California', In: 'Geomorphic processes and aquatic habitat in the Redwood Creek drainage basin', *U. S. Geologic Survey Professional Paper*, U. S. Government Printing Office, Washington, D. C.

Redpath, B. B. 1973. *Seismic Refraction Exploration for Engineering Site Investigations, Technical Report* **E-73-4**, *U. S. Army Engineer Waterways Experiment Station Explosive Excavation Research Laboratory*, Livermore, CA, 51 pp.

Sheriff, R. E. and Geldart, L. P. 1982. *Exploration Seismology Volume 1: History, Theory, and Data Acquisition.* Cambridge University Press, Cambridge, England, 253 pp.

Stewart, R. and Peselnick, L. 1977. 'Velocity of compressional waves in dry Franciscan rocks to 8 kilobar and 300 C.', *J. Geophys. Res.*, **82**, 2027-2039.

Swanston, D. N., Ziemer, R. R., and Janda, R. J. 1983. *Influence of Climate on Progressive Hillslope Failure in Redwood Creek Valley, Northwestern California, U.S. Geological Survey Open-File Report* **83-259**, U. S. Government Printing Office, Washington, D. C., 42 pp.

Trantina, J. A. 1962. 'Investigation of landslides by seismic and electrical resistivity methods', In: *Field Testing of Soils, ASTM Special Technical Publication No. 322*, Philidelphia, PA, 120-134.

Ziemer, R. R. 1984. 'Response of progressive hillslope deformation to precipitation', In: *Proc. Symposium on Effects of Forest Land Use on Erosion and Slope Stability, 7-11 May, 1984, Honolulu, Hawaii*, C. L. O'Loughlin and A. J. Pearce, eds., Environment and Policy Institute, East-West Center, University of Hawaii, Honolulu, Hawaii, 91-98.